Multi-Source Renewable Energy Exchange Management System for Off-Grid Home Load

Samir Arfa*, Mohsen Ben Ammar*‡, Mohamed Ali Zdiri*, Hsan Hadj Abdallah*

* University of Sfax, National Engineering School of Sfax, Control and Energy Management Laboratory, (CEMLab), BP 1173, Sfax, 3038, Tunisia.

(samir.arfa@enis.tn; mohsen.benammar@enis.tn; mohamed-ali.zdiri@enis.tn; hajabdallahhsan@gmail.com)

‡ Corresponding Author; Mohsen Ben Ammar, ENIS, University of Sfax, Tunisia.

Tél: +216 70 258 520 Fax: +216 74 275 595. E-mail: mohsen.benammar@enis.tn

Received: 21.07.2022 Accepted: 04.09.2022

Abstract- Green and ecological energy sources are nowadays promising power sources, effectively useful for electrifying regions sited far away from the electricity grid. In this context, the current work proposes an advanced energy management strategy in which an isolated domestic site could be fed by a multi-source site supply. The multi-source system includes a WT coupled to a PMSG permanent magnetic synchronous generator, a solar PV, a storage battery, a diesel generator as a power generation system, AC load, and dump load. Basically, the advanced management strategy rests on the idea of equating the wind turbine and photovoltaic generator provided energy and the domestic load required energy. To ensure the home-provided electrical energy autonomy, we consider implementing a special battery charge/discharge storage system, as well as a diesel generator used as a backup source, in case of a lack of renewable energy sources and minimal battery state of charge (SOC). In this context, our major aim consists mainly in boosting the studied system's energy management strategy (EMS), through ensuring constant frequent supply and maintaining it to meet the variable daily (24-hour) consumption. In order to prevent power losses, a dump load as an auxiliary load is used in case of excess renewable power. The efficiency of the advanced energy-management strategy was actually tested and verified under all possible operating conditions. The achieved results turn out to confirm the scheme's reliability in maintaining harmonious synchronization between energy production and consumption processes, in terms of system autonomy and power-loss minimization.

Keywords Wind turbine; photovoltaic generator; storage battery; diesel generator; energy-management system.

1. Introduction

Throughout the past decade, electricity production has demonstrated a significantly sharp challenge [1]. Indeed, the world's electric energy production proves to rest predominantly on fossil-fuel based sources, whose intensive consumption has resulted in massive greenhouse gas emissions, thereby, further aggravating the pollution phenomenon [2,3], and seriously threatening the environment. Additionally, extreme and extravagant natural energy consumption has engendered an emanating reduction in these reserves, heading towards depletion, or exhaustion. Alternatively, however, renewable energy sources have nowadays occupied an important position in the field of electricity production, due mainly to their availability and reliability [4-6]. In this respect, several works have been conducted to investigate the issue of renewable energy sources, particularly the wind and photovoltaic based energy [7], characterized as practically abundant inexhaustible electrical resources, relative to fuel energy, and particularly concentrated in determined regions. In this regards an effective protection against the aggravating threat of pollution, stand-alone renewable power systems turn out to represent attractive ecological solutions, useful for implementation as appropriate rural electrification schemes [8-11]. The stand-alone renewable power systems are particularly intended for installation in rural areas located far away from the reach of the general electrical grid.

Concerning our particular study context, and for the purpose of constructing an equitably effective domestic load profile, an appeal is made to the online application of the Tunisian Electricity and Gas Company (STEG) [12], to help us draw an aggregated domestic load profile. In effect, the existing loads profiles are already used in several energy

management applications [13] that rely on estimating the STEG subscribers' consumption history. As regards the second part of our research, it is devoted to the developing and managing a multi-source renewable energy generation framework incorporating photovoltaic and wind power generators, as well as a battery, diesel generator (DG) and dump load.

It is worth noting, in this context, that the aim behind conducting the present work consists mainly in developing a special management scheme, whereby, energy could be autonomously supplied to a domestic dwelling sited far away a long distance from the already existing electric grid. The main objective is to provide the domestic load with the required power supply, necessary for carrying out the relevant household activities and accomplishing daily routines. Should the renewable energy sources' generated power turn out to be lower than the load energy requirement, an initial appeal is made to the batteries' stored energy. Once it proves to be still insufficient, we then resort to applying the emergency diesel generator. Still, in case the load energy is discovered to be lower than the renewable energy sources' supplied power, the applied batteries would then resume the charging process. When the batteries are fully charged, the energy excess is then transferred to the auxiliary load (dump). In absence of renewable energy sources, however, we undertake, in the first stage, to apply the batteries' energy supply, prior to subsequently using the diesel generator provided power.

Actually, studies dealing with the subject of permanent multi-source system design are numerous. Indeed, several management strategies have been developed and advanced in the relevant literature with the aim of maintaining the PV system's permanent continuity and reliability. In this regard, several researchers have considered elaborating on the idea of hybrid energy management systems (wind and PV sources) and storage designs (batteries). However, the existing energy management schemes appear to display noticeable drawbacks. For instance, they do not seem to account effectively for such conditions as the absence of renewable energy sources in unfavourable situations (i.e., the absence of sunlight at night concerning photovoltaic energy, as well as the absence of wind and discharge regarding the batteries) [14]. To resolve these problems, therefore, we consider it useful to implement a diesel generator fit for installation in the renewable-energy dependently isolated domestic sites, to serve as a backup unit in case of the other energy sources' deficiency. In the case when the generated renewable-energy power appears to exceed the domestic load power capacity, however, an auxiliary load is incorporated to help absorb the energy excess once the battery is completely charged. It is worth noting, in this context, that this novel process, or solution, has never been actually treated by most of the existing research works.

The remainder of this work comprises eight sections, organized as follows. After the introduction, Section 2 provides a depiction of the advanced multi-electrical source system. The suggested system's control process modelling is subject of section 3. As for section 4, it is devoted to depicting the various relevant electronic converters and control techniques, while section 5 outlines the proposed method's details, as adapted to implement a real load profile fit for installation in isolated sites [15]. Concerning section 6, it is dedicated to the development of a special energy management strategy, whereby, effective energy distribution among the multi-source system various components can be maintained. The study achieved simulation results and relevant discussions are depicted in section 7, and section 8 involves the main concluding remarks.

2. The Study Advanced System

Fig. 1 depicts the investigated standalone multi-source system. It includes a WT coupled to a PMSG permanent magnetic synchronous generator, a solar PV, a storage battery, a diesel generator as a power generation system, AC load, and dump load [16].

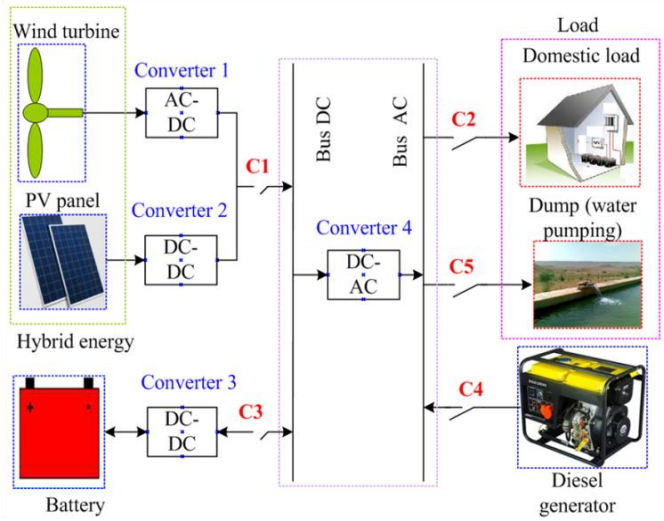

Fig. 1. The suggested system's architecture.

The wind turbine, PV and battery are linked to a DC bus via three power converters. An AC-DC converter is placed in the generator terminal to maintain control of the WT variable speed motion. The system also involves a bi-directional DC-DC converter, enabling to manage the battery emanating power flow during a power shortage or excess affecting the entire system. At this junction, a diesel generator, linked to the power system via an AC bus, is applied as a backup power system. It serves to supply the domestic load in case of the renewable energy sources' deficiency.

3. Isolated Site Modelling

3.1. Wind Turbine Generator

The wind kinetic energy, with variable speed, strikes the wind turbine blades to generate mechanical energy, then transformed into electrical energy by means of a PMSG. The WT-generated mechanical power is proportional to the wind speed cube. Expression of the wind mechanical power, as provided by [17], is:

$$P_W = \frac{1}{2} C_{PW} . \rho . \pi . R_W^2 . V_W^3 \quad (1)$$

Where: C_{PW} denotes the power coefficient describing the wind turbine performance; ρ represents the air density ($kg.m^{-3}$); R_W stands for the wind-turbine rotor radius (m), and V_w designates the wind speed in $m.s^{-1}$.

Specific speed is the peripheral speed ratio of the turbine brought back at the wind speed, as expressed by [18]:

$$\lambda = \frac{R_W \Omega}{V_w} \tag{2}$$

Where: Ω represents the wind-turbine rotor speed.

Applying the Park transformation, the PMSG voltage in the dq frame is provided by the following equations [19]:

$$V_{sd} = R_s I_{sd} + L_s \frac{d_s I_{sd}}{dt} - p\Omega L_s I_{sq} \tag{3}$$

$$V_{sq} = R_s I_{sq} + L_s \frac{d_s I_{sq}}{dt} + p\Omega L_s I_{sd} + p\Omega \phi_m \tag{4}$$

Relying on the fundamental dynamic relationship, evolution of the turbine rotation speed is determined by:

$$J \frac{d\Omega}{dt} = T_m - T_{em} \tag{5}$$

Where: T_m is the wind output torque, and T_{em} represents the electromechanical torque.

3.2. PV Generator Modeling

The PV effect, as applied in solar cells, allows the direct conversion of light energy emanating from solar rays into electricity. The PV cell equivalent electrical model is illustrated in Fig. 2, below.

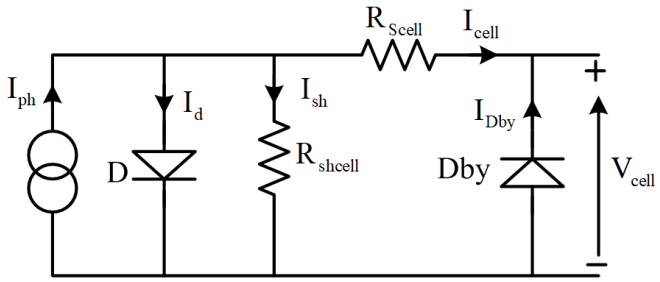

Fig. 2. PV cell equivalent electric circuit.

With: I_{ph} denotes photocurrent, practically proportionate to G solar radiation. It is worth noting that the PV cell current is obtained by the following equation [20]:

$$I_{cell} = I_{ph} - I_s \left[\exp\left(\frac{V_{cell} + R_{Scell} I_{cell}}{V_T} \right) - 1 \right] - \frac{V_{cell} + R_{Scell} I_{cell}}{R_{Shcell}} \tag{6}$$

Where: I_s represents the diode saturation current (A), and R_{Shcell} models the cell(Ω) flowing parasitic currents, while R_{Scell} models the material (Ω) ohmic losses, and V_T designates the thermo-dynamic voltage.

The PV cell power and PV generator are respectively depicted through the following equations:

$$P_{cell} = I_{cell} V_{cell} \tag{7}$$

$$P_{gpv} = N_{sm} N_{pm} I_m V_m \tag{8}$$

Where: I_{cell} and V_{cell} respectively designate the PV cell current and voltage; N_{sm} denotes the panel number in series; N_{pm} represents the number of PV strings, while I_m and V_m are, respectively, the PV module current and voltage.

3.3. Battery System Modeling

Concerning the present study, a lead-acid type of battery [21], connected to the direct-current bus via a DC/DC converter, is used. The battery model is necessary for estimating the SOC, as illustrated in Fig. 3, below:

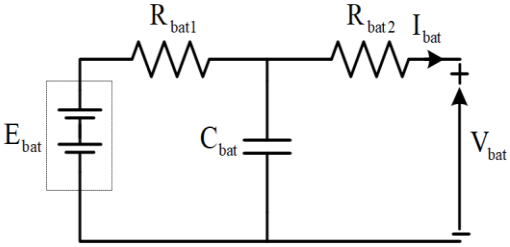

Fig. 3. Battery model circuit.

With: E_{bat} represent the open-circuit voltage; R_{bat1} and R_{bat2} are the battery internal resistances; C_{bat} is the capacitor; I_{bat} and V_{bat} denote the battery current and voltage, respectively.

It is worth noting, in this context, that a lead acid battery has been utilized to store the excess energy of the renewable electrical energy sources. The battery power is depicted by the equation (9), below [22]:

$$Q_{bat} = Q_{bat-i} + \int_0^t V_{bat} I_{bat} dt \tag{9}$$

Where: Q_{bat-i} is the initial value charge; I_{bat} and V_{bat} are the battery current and voltage, respectively. The battery capacity, DOD and SOC are expressed by the equations (10), (11), and (12), respectively:

$$C_R(t) = C_R(t-1) + \frac{\partial t}{3600} I_{bat}^{kp} \tag{10}$$

$$DOD(t) = 100 - SOC(t) \tag{11}$$

$$SOC(t) = \frac{C_R(t)}{C_p} \tag{12}$$

Where: ∂t denotes the time difference; DOD represents the depth of discharge; C_P is the Peukert capacity; I_{bat} designates the battery current, and k_p is the Peukert constant.

3.4. Boost Converter Modeling

For an effective adaptation of the PV and the other systems, a DC-DC converter has been applied. Control of the converter is strictly maintained to ensure a constant DC voltage level. The boost converter associated electrical circuit is depicted in Fig. 4 [23]:

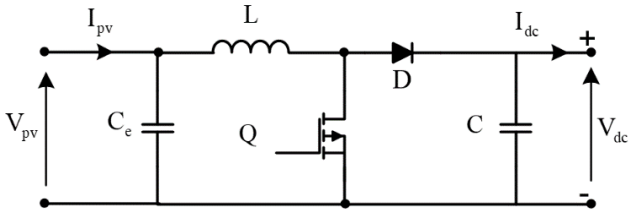

Fig. 4. The boost converter's electrical model.

The DC bus voltage (output voltage) is expressed by a function of the PV voltage, such as:

$$V_{dc} = \frac{V_{pv}}{1\text{-}d} \tag{13}$$

With d is the duty cycle.

3.5. The DC/DC Converter Modeling

The Buck Boost converter is a device that serves to convert energy from a direct current voltage to a variable direct current voltage. Fig. 5, below, outlines the DC/DC converter connected electrical circuit.

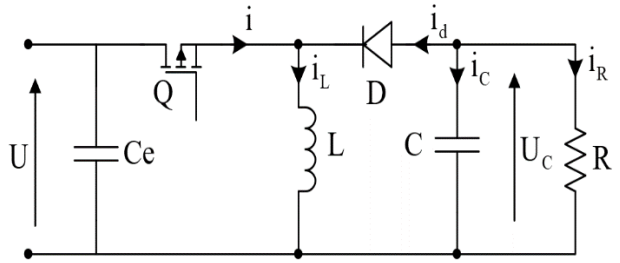

Fig. 5. Electrical model of the Buck-Boost converter.

Like the buck converter and boost converter, the operating principle of this converter could be drawn based on the Q switch Buck-Boost converter's closed and open states. Table 1, below, illustrates the various DC/DC converters associated parameters.

Table 1. Numerical calculation of the parameters of the different converters' topologies considered.

	Boost	**Buck-boost**
$G_v(d)$	$\frac{1}{1-d}$	$\frac{d}{1-d}$
L	$\frac{d_m V_m}{f\Delta I_L}$	$\frac{d_m V_m}{f\Delta I_L}$
C_e	$\frac{d_m V_m}{8L\Delta V_m f^2}$	$\frac{(1-d_m) I_m}{2\Delta V_m f}$
C	$\frac{d_m I_{S_m}}{f\Delta V_{S_m}}$	$\frac{d_m I_{S_m}}{f\Delta V_{S_m}}$

3.6. DC/AC Converter Modeling

For a thorough analysis of the electric-power generating system's dynamic behaviour, a full-system equivalent modeling needs to be developed, to highlight the critical importance of DC/AC modeling in the Park reference. Accordingly, the modulated voltages of the inverter are provided by the equations (14) and (15), below [24]:

$$V_{md} = K_d \frac{V_{dc}}{2} \tag{14}$$

$$V_{mq} = K_q \frac{V_{dc}}{2} \tag{15}$$

Where: K_d and K_q designate the converter control voltages' direct and quadrature components, respectively.

3.7. Diesel Generator Modelling

The DG is designed to serve as an emergency-use electric generator. It incorporates a diesel engine connected to a PMSG, and is used in several industrial applications [25]. It is actually conceived to ensure the load demand during periods of renewable energy sources' unavailability, and storage systems' energy insufficiency. Accordingly, the generator is modelled and sized by a first-order transfer function system, enabling to maintain a power rate P_{DG} equal to 5kW.This diesel generator is illustrated in Fig. 6, below.

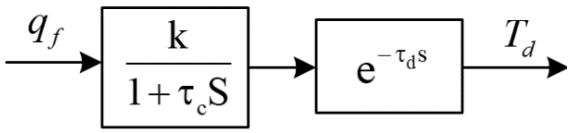

Fig. 6. The diesel generatorelectrical modeling.

With: τ_d designates the start delay, k is the gain and τ_c the time constant.

3.8. The Filter's Electrical Model

The filter applied in this study is depicted through the following figure [26]:

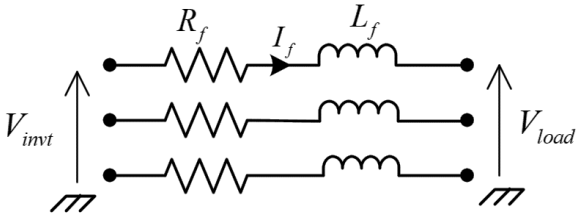

Fig. 7. Electrical model of the filter.

Where: R_f denotes the filter resistance, and L_f is the filter inductance.

Following the park transformation, the filter associated system of equations is provided by the following equations:

$$V_{invt\_d} = R_f I_{fd} + L_f \frac{dI_{fd}}{dt} - L_f \omega t I_{fq} + V_{load\_d} \tag{16}$$

$$V_{invt\_q} = R_f I_{fq} + L_f \frac{dI_{fq}}{dt} + L_f I_{fd} + V_{load\_q} \tag{17}$$

4. Control of the applied converters

1.1. The P&O MPPT Technique

In order to supply the load with maximum electrical power, several techniques have been developed, mainly, the perturbation and observation (P&O) technique, the incremental conductance method, along with the fractional SCC and fractional VCO techniques [27].

The P&O method is widely used in PV systems owing to its remarkable simplicity. It rests on the principle of transaction between perturbation and observation until MPP is actually attenuated. The below-figuring algorithm highlights the P&O MPPT technique outlines [28].

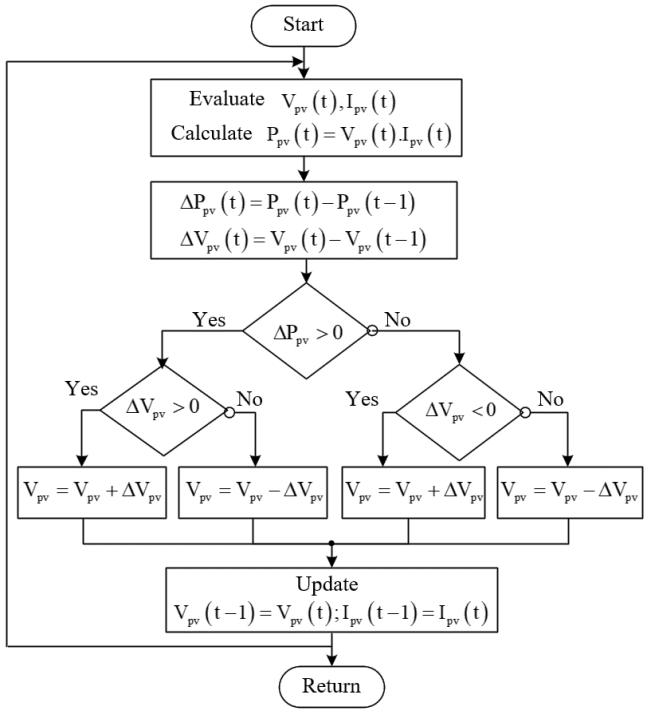

Fig. 8. The P&O MPPT technique organigram.

1.2. PQ Control of the Inverter

It is maintained via the droop control method, a rather robust and simple to implement technique, as highlighted in Fig. 9, below [29]:

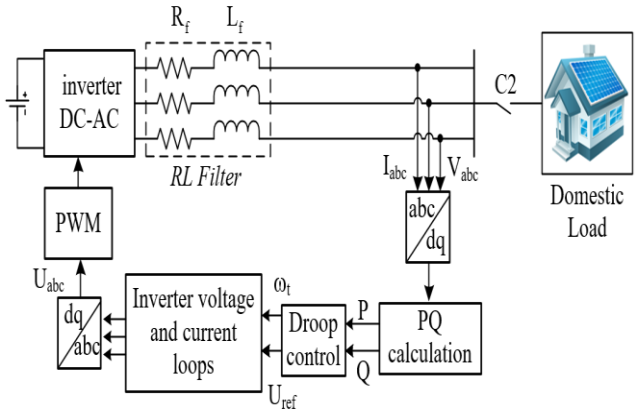

Fig. 9. The PQ control technique.

Mathematical modeling of the droop control technique is provided by the following process:

$$\begin{cases} P_{inv} = \frac{3}{2}\left(V_d.I_d + V_q.I_q\right) \\ Q_{inv} = \frac{3}{2}\left(V_d.I_q - V_q.I_d\right) \end{cases} \quad (18)$$

Once the direct current is equal to zero (I_d= 0), the active and reactive power relevant equations turnout to be:

$$\begin{cases} P_{inv} = \frac{3}{2}V_q.I_q \\ Q_{inv} = \frac{3}{2}V_d.I_q \end{cases} \quad (19)$$

5. The Real Domestic Load Profile Relevant Methodology

This section is dedicated to the setting up of a domestic load profile fit for application in isolated site. It is worth mentioning, in this respect that, the Tunisian Electricity and Gas Company (STEG) has already devised an online application, dedicated to estimating the bi-monthly bill (two months), in a bid to maintain a highly reliable load profile [12]. By filling in and analysing the relevant data, this application helps in computing the estimated electricity usage ends. Table 2, below, displays the household energy applied purposes and consumption rates, as maintained by our designed architecture, for an isolated site

Table 2. Household electrical load.

Devices	Nber	Usage duration	Consumption rate
Lighting	8	3h	13 %
Refrigerator	1	24 h	29 %
TV/Radio	1/1	4/2 h	8 %
Microwave and oven	1	3 h	4 %
Washing machine	1	2 h	2 %
Ironing machine	1	1 h	5 %
Heating /Air conditioning	1	2/3 h	29 %
Personal Computer	1	2 h	7 %
Various equipment	5	2 h	3 %

The bi-monthly power consumption percentage (%) is illustrated by the pie chart (Fig. 10), below.

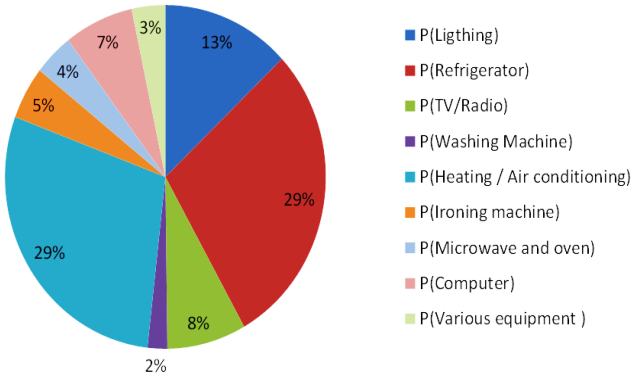

Fig. 10. Domestic load consumption percentage.

The actual domestic-load consumption application corresponding curve is illustrated through Fig. 11, below.

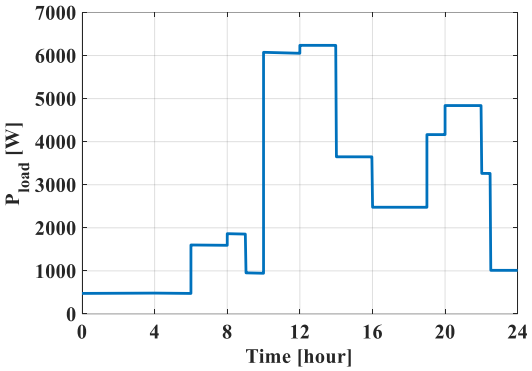

Fig. 11. Domestic power load.

Our advanced standalone multisource electrical system rests heavily on the domestic load power requirement, likely to guarantee a reliable amount of energy. The isolated-site load power profile, as applied in our study case, ranges between [0,5 kw] and [6,8 kW]. As highlighted in Fig. 11, the domestic usage profile usually witnesses three daily peak periods. First, a small peak morning period, associated with the routine morning activities [30]. It is followed with a high afternoon peak period, then, a medium peak evening period. The midday and evening peaks are associated with such frequent activities as dinner preparation, home lighting, TV watching and entertainment.

6. Power Management for an Isolated Site "Multi-Source Autonomous System"

Power management represents an important stage in the isolated site supply process. For this purpose, we consider developing a special power management strategy useful for monitoring the power transfer process among the different devices making up the system's architecture [14]. Furthermore, several power management strategies have been applied to multiple systems as presented in [31-34]. To ensure that energy is efficiently delivered to the domestic load, the design must be apt to maintain effective control and management of the various energy sources incorporating a WT coupled to a PMSG permanent magnetic synchronous generator, a solar PV, a storage battery, along with a diesel generator. Hence, for an effective practical management strategy to take place, a critical set of relevant criteria must be satisfied and pursued, as illustrated in Fig. 12 [28].

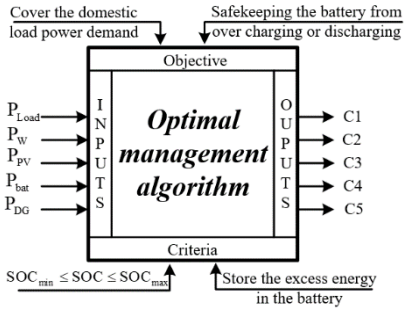

Fig. 12. A block diagram of the management algorithm suggested.

The system's energy management strategy (EMS) is highlighted in Fig. 13, below.

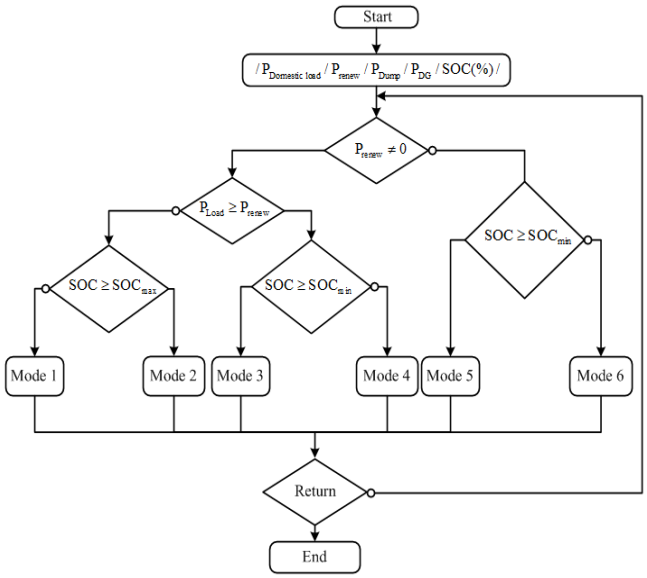

Fig. 13. The system's energy management strategy.

Description of the proposed EMS involves the following main steps:

Step 1: defining the various power sources involved in the hybrid electrical system's architecture.

Step 2: once the hybrid system's power supply appears to exceed the domestic load's power requirement, two modes are possible:

Mode 1: in the case when the battery charge state is lower than the maximum level, the power excess is then transformed to the battery $\left(P_{renew} = P_{load} + P_{bat}\right)$.

Mode 2: in case the battery SOC appears to exceed the SOC_{max} level, the energy excess is then transferred to the auxiliary domestic load $\left(P_{renew} = P_{laod} + P_{Dump}\right)$.

Step 3: if the domestic load power turns out to exceed the generated power amount, two cases would ensue:

Mode 3: if the battery SOC is higher than SOC_{min}, the battery will then undertake to supply the domestic load $\left(P_{load} = P_{renew} + P_{bat}\right)$.

Mode 4: otherwise, the battery will be disconnected from the system, and the diesel generator will then intervene to compensate for the power needed.

Step 4: if the wind turbine and photovoltaic generated energy are equal to zero, two states are imposed:

Mode 5: when the battery is charged, it will start to supply the domestic load $(P_{load} = P_{bat})$.

Mode 6: when the battery is fully discharged, the diesel generator will ensure the power supply autonomously $(P_{load} = P_{DG})$. It is to be highlighted that the diesel generator is used to supply the load in case of emergency.

7. Simulation Results

The Simulink model of the proposed system is shown in Fig. 14. In this section, highlights of the wind speed and DC link voltage drawn simulation results are depicted, along with the system's power-generation management design. The Matlab/Simulink executed simulation has been administered on a 24-hour basis.

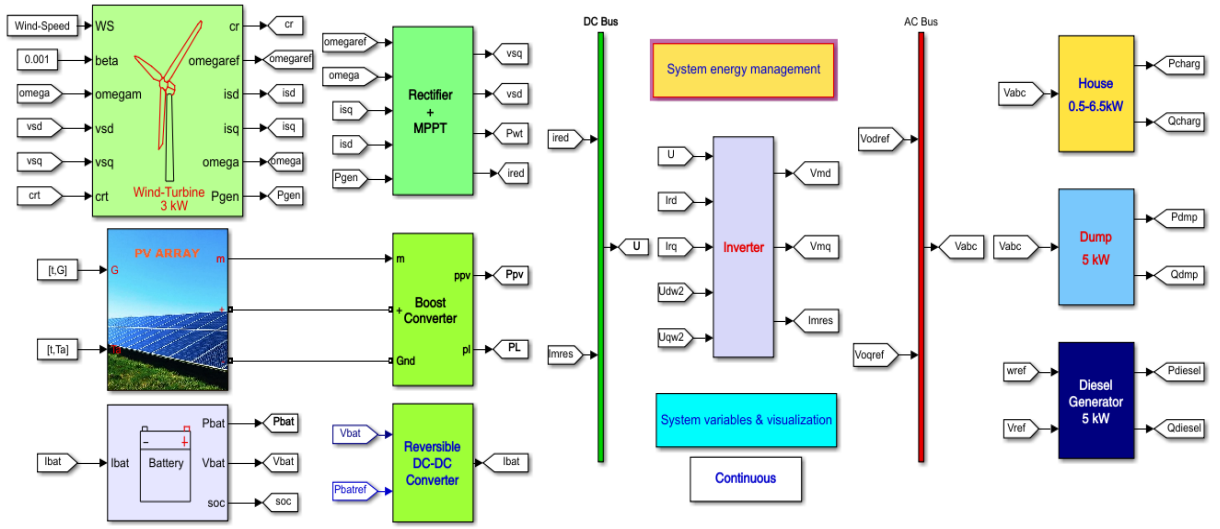

Fig. 14. Matlab simulink model of the system studied.

The PV array characteristics are displayed in Fig. 15, below.

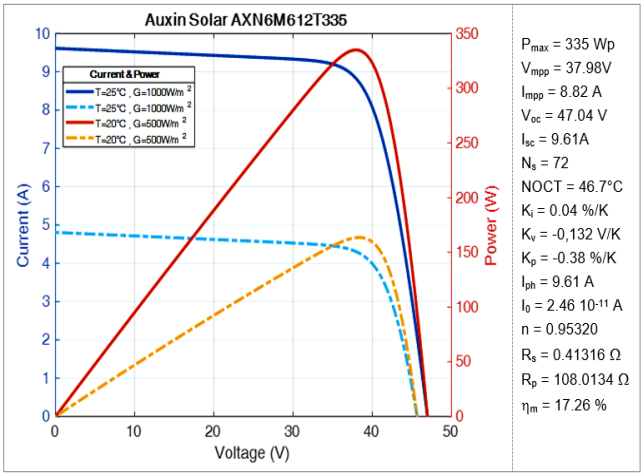

Fig. 15. PV Array characteristics.

The PMSG parameters, DC-DC converter, battery parameters and diesel generator are respectively represented on Tables 3, 4, 5 and 6 below:

Table 3. The PMSG and filter respective parameters.

Description	Value
P (Rated power in kW).	3
J (Moment of inertia in kg.m^2).	99.10^{-4}
p (Number of pole pairs)	4
R_s (Resistor in Ω).	0.82
L_s (Stator inductance in H).	15.10^{-3}
F (Friction factor in N.m.s.rad^{-1})	10^{-3}
Φ_m (Magnetic flux of magnets in Wb)	0.5
R_f (Filter resistance in mΩ)	100
L_f (Filter inductance in mH)	3

Table 4. DC-DC converter.

	Boost	Buck-boost
C_e (Input capacitor in µF)	50	50
C (Output capacitor in µF)	3300	3300
L (Inductance in mH)	1	2
f (Switching frequency in kHz)	10	10

Table 5. Battrey parameters.

Description	Value
P_{bat} (Rated power in kW)	4
I_{bat} (Battery current in A)	15
q_{bat} (Battery capacity in Ah)	150

Table 6. Diesel Generator parameters.

Description	Value
P_{DG} (Rated power in kW)	5
τ_c (Delayed combustion of fuel oil in s)	0.2
τ_d (Start delay in s)	0.003
Ω_{dg} (Rated speed in rad/s)	157

Highlights of the wind speed variations are depicted in Fig. 16, below.

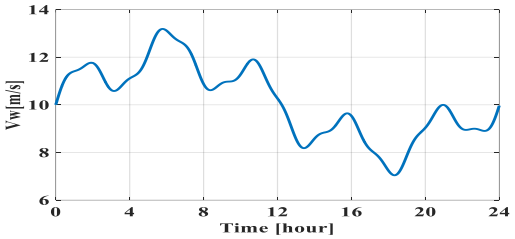

Fig. 16. Wind speed variations.

The real profile used of the solar radiation and temperature is represented by the following figure.

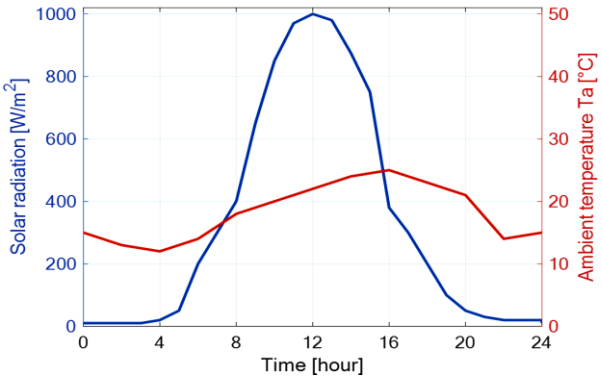

Fig. 17. Solar radiation and temperature variations.

The system's DC bus voltage set is adjusted to 550 V, as highlighted in the following chart.

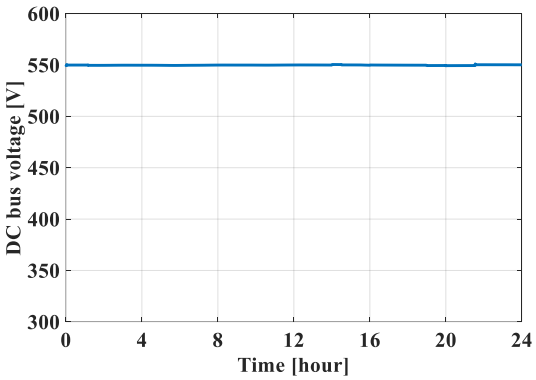

Fig. 18. DC bus voltage.

It is worth noting that the main idea developed in this work is that the PV generator is made operable only during the day, due to the absence of sun at night, as illustrated in Fig. 19 with P_i representing the power of the PV, wind or both sources. Still, the developed system is naturally expected to operate on a whole-day basis (24 hours). Renewable energy sources, as generated by the wind and photovoltaic sources, are provided by the following equation:

$$P_{renew} = P_{PV} + P_W \quad (20)$$

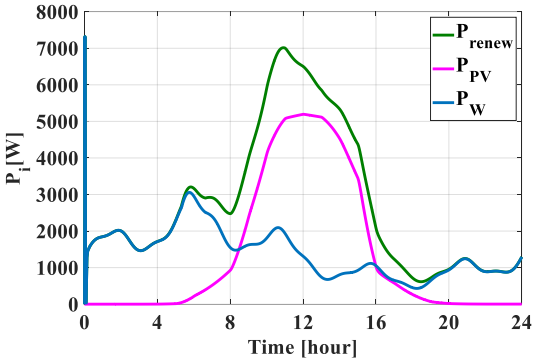

Fig. 19. Renewable energy sources'generated power.

The standalone system generated energy and domestic load power requirement are presented in Fig. 20. This figure, which illustrates the results of the advanced system power management as follows:

- From time 0 to t1, t3 to t4 and t7 to 24 h:

  $P_{renew} > P_{load}$, case in which, the power excess is stored in the battery.

- From time t1 to t2 and t4 to t5: $P_{renew} > P_{load}$ and the battery is almost charged. At this level, the dump load absorbs the excess energy.

- From time t2 to t3 and t5 to t6: In this case,

  $P_{renew} < P_{load}$ and $SOC > SOC_{maxin}$. The photovoltaic, wind turbine and battery jointly provide energy to supply the domestic load.

- From time t6 to t7: At night, the renewable energy power is lower than the load requested energy and the $SOC < SOC_{min}$ .In this case, the diesel generator ensures the power supply of the domestic load.

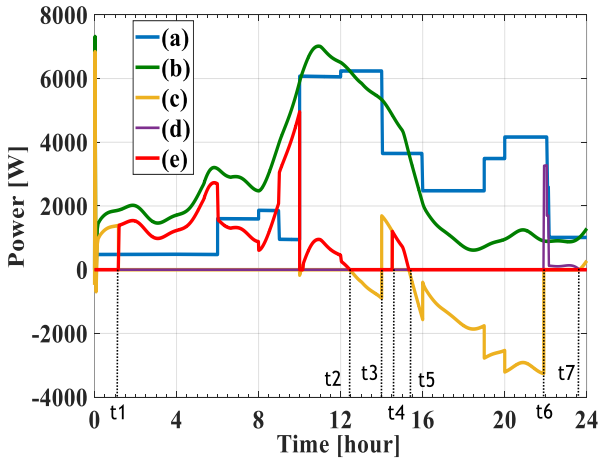

Fig. 20. The stand-alone power system. Legend: (a): domestic load power; (b): renewable-energy sources' power; (c): battery power; (d): diesel generator power, and (e): dump power.

The switches' evolving states (C1, C2, C3, C4, and C5) are represented in Fig. 21. Accordingly, one could maintain that the diesel generator is made to operate only when the battery

is fully discharged, i.e., in the case of total lack of renewable energy.

The excessive energy state, in which the dump load starts to absorb the energy surplus over the whole day, occurs when the renewable sources prove to produce energy at high levels and the battery's charge state is maximized, as illustrated in Fig. 20.

It is only in case of renewable energy and battery power failures, however, that the diesel generator is triggered to operate. The battery SOC is highlighted in Fig. 22.

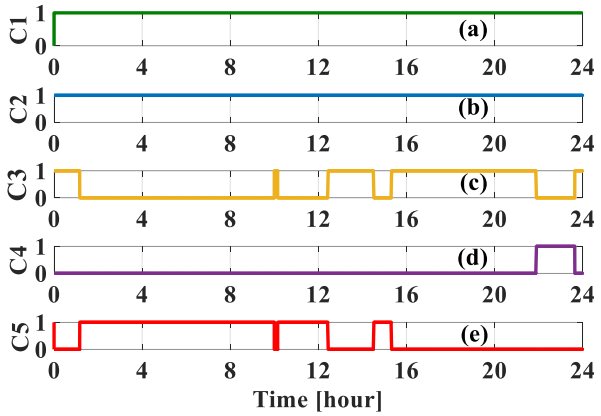

Fig. 21. The switches states. Legend: (a): C1; (b): C2; (c): C3; (d): C4, and (e): C5.

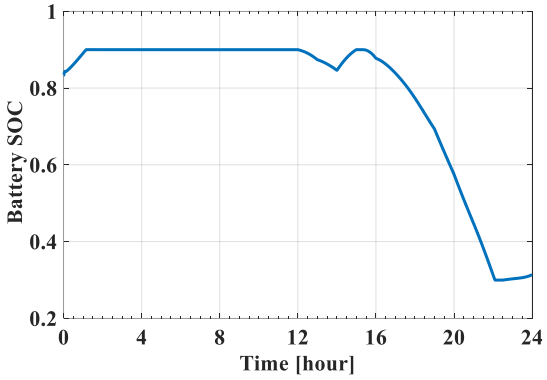

Fig. 22. The battery SOC evolving levels.

Based on Fig. 22, the battery stored energy turns out to be predominantly used during a specified day period. This would allow us to pinpoint effectively the battery charge/discharge cycle, likely to affect the entire system's life span and durability aspects.

Regarding the load output voltage, as illustrated in Fig. 23, one could well ensure that the voltage is constantly maintained on a whole day basis, whatever the climatic condition variations might be. Thus, the advanced energy-management scheme associated performance and high efficiency prove to testify well the system's robustness, mainly in terms of autonomy and self-sufficiency.

Thus, through conducting the present work, we have been able to successfully satisfy the domestic load energy demand by effectively maximizing the use of renewable energy sources, while maintaining an efficient storage capacity. We have managed to resolve the problem of excessive energy supply by incorporating the dump mechanism solution. Noteworthy, however, is that the battery use is generally restricted to the night lapse, due to the absence of sun rays. Similarly, the diesel generator's use turns out to be very limited (just at night), following the battery's complete discharge. In conclusion, the proposed energy management strategy ensures the balance between production and consumption taking into account these variations, which guarantees the stability of our system.

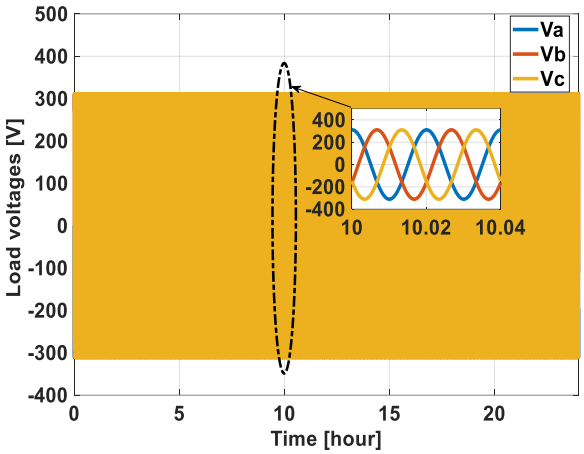

Fig. 23. The load voltage output.

8. Conclusion

Throughout the scope of the present work, effort has been devoted to design and set up a novel domestic-load energy profile, effectively monitored at various intervals, possible circumstances and situations. To this end, appeal has been made to the Tunisian Electricity and Gas Company application of online usage-estimation. Then, the domestic electrical loads and usage modes have been introduced.

Subsequently, a special management algorithm is put forward to develop a hybrid multi-source system (wind and photovoltaic sources) that incorporates a battery based storage system, along with a DG type of backup source for emergency use purposes. This energy management design is intended for application as a domestic load supply framework for households sited far away from the public grid reach, to maintain continuous electricity generation and provision. To this end, a dump load has been incorporated into the system, to absorb the energy excess once the generated power turns out to exceed the domestic load capacity, and the battery is fully charged.

Regarding the power balance dimension, however, it is developed and managed in such a way as to follow the domestic-load variable power pace. Indeed, judging by the attained simulation results, achieved while accounting for the climatic conditions and monitoring load variations, the proposed energy-management strategy turns out to demonstrate a remarkable performance and high efficiency in terms of system continuity and power-loss prevention.

Appendix

EMS: Energy Management Strategy

MPP: Maximum power point

MPPT: Maximum power point tracking
PMSG: Permanent Magnetic Synchronous Generator
SOC: State Of Charge
PV: Photovoltaic
C: Output capacitor (μF)
C_e: Input capacitor (μF)
C_{PW}: Wind turbine power coefficient
d: Duty cycle
d_m: Duty cycle at MPP
G: Solar radiation (W/m^2)
G_v: Voltage Gain
I_{Dby}: Bypass diode current (A)
I_{rs}: Cell reverse saturation current (A)
I_s: Diode saturation current (A)
I_{ph}: Photocurrent (A)
I_{pv}: Photovoltaic current (A)
I_{sd}, I_{sq}: Stator currents in Park frame (A)
I_m: PV current at MPP (A)
I_{sm}: Output current at MPP (A)
I_d, I_q: Inverter currents in Park frame (A)
I_{fd}, I_{fq}: Filter currents along d and q axis (A)
L_{sd}, L_{sq}: Stator winding inductance (H)
P_w: Wind power (W)
P_{pv}: Photovoltaic power (W)
P_{inv}: Inverter power (W)
P_{renew}: Renewable power (W)
P_{DG}: DG power (W)
Q_{inv}: Inverter power (W)
q_F: Fuel flow
R_m: Equivalent resistance at MPP (Ω)
R_{Scell}: PV cell series resistance (Ω)
R_{Shcell}: PV cell shunt resistance (Ω)
R_s: Stator winding resistor (Ω)
R_W: Blade length (m)
s: Laplace operator
SOC_{max}: Maximum state of charge (%)
SOC_{min}: Minimum state of charge (%)
T: Ambient temperature (°C)
T_d: Resistive torque (N.m)
T_m: Wind output torque (N.m)
$T_{em:}$ Electromechanical torque (N.m)
U: Input voltage Buck-Boost converter (V)
Uc: Output voltage Buck-Boost converter (V)
V_W: Wind speed (m/s)
V_{sd},V_{sq}: Stator voltages in Park frame (V)
V_d and V_q: Inverter voltages in Park frame (V)
V_m: PV voltage at MPP (V)
V_{sm}: Output voltage at MPP (V)
V_{pv}: PVvoltage (V)
V_{inv}: Inverter voltage (V)
V_{load}: Load voltage (V)
ΔP_{pv}: PV power variation (W)
ΔV_{pv}: PV voltage variation (V)
ΔVs_m: Output voltage ripple amplitude (V)
ΔV_m: Voltage ripple amplitude (V)
ΔI_L: Current ripple amplitude (A)
ρ: Air density (kg/m^3)
Ω: Angular speed (rad/s)
ω_t: Pulsation (rad/s)

References

[1] A. Shaqour, H. Farzaneh, Y. Yoshida, and T. Hinokuma, "Power control and simulation of a building integrated stand-alone hybrid PV-wind-battery system in Kasuga City, Japan", Energy Reports, vol. 6, pp. 1528-1544, 2019.

[2] Y. Zhang, H. Sun, and Y. Guo, "Integration Design and Operation Strategy of Multi-Energy Hybrid System Including Renewable Energies, Batteries and Hydrogen", Energies, vol. 13, 5463, 2020.

[3] N. Yimen, T. Tchotang, A. Kanmogne, and I. A. Idriss, "Optimal Sizing and Techno-Economic Analysis of Hybrid Renewable Energy Systemsa Case Study of a Photovoltaic/Wind/ Battery/ Diesel System in Fanisau, Northern Nigeria", Processes, vol. 8, 1381, 2020.

[4] A. Razmjoo, R. Shirmohammadi, A. Davarpanah, F. Pourfayaz, and A. Aslani, "Stand-alone hybrid energy systems for remote area power generation", Energy Reports, vol. 5, pp. 231-241, 2019.

[5] U. R. Nair, and R. Costa-Castello, "A Model Predictive Control-Based Energy Management Scheme for Hybrid Storage System in Islanded Microgrids", IEEE access, vol. 8, pp. 97809-97822, 2020.

[6] P. Kumar, R. Chandrasena, V. Ramu, G. Srinivas, K. V. S. M. Babu, "Inertia emulation control technique based frequency control of grid-connected single phase rooftop photovoltaic system with battery and supercapacitor", IET Renewable Power Generation, vol. 7, pp. 1156-1163, 2020.

[7] P. Kumar, R. Chandrasena, V. Ramu, G. Srinivas, K. V. S. M. Babu, "Energy Management System for Small Scale Hybrid Wind Solar Battery Based Microgrid", DOI:10.1109/ACCESS.2020.2964052, IEEE Access, vol. 8, pp. 8336-8345, 2020.

[8] D. Icaza, D. B. Diez, S. P. Galindo, and C. F. Vázquez, "Modeling and Simulation of a Hybrid System of Solar Panels and Wind Turbines for the Supply of Autonomous Electrical Energy to Organic Architectures", Energies, vol. 13, 4649, 2020.

[9] A. Abdelkafi, A. Masmoudi, and L. Krichen, "Assisted power management of a stand-alone renewable multi-

source system", Energy, doi: 10.1016/j.energy.2017.12. 133, vol. 145, pp. 195-205, 2018.

[10] A. Abdelkafi, A. Masmoudi, and L. Krichen, "Experimental investigation on the performance of an autonomous wind energy conversion system", International Journal of Electrical Power & Energy Systems, vol. 44, no. 1, pp. 581-590, 2013.

[11] K. Ghaib, and F.Z. Ben-Fares, "A design methodology of stand-alone photovoltaic power systems for rural electrification", Energy Conversion and Management, 148, pp. 1127-1141, 2017.

[12] M. B. Ammar, M. Chaabene and A. Elhajjaji, "Daily energy planning of a household photovoltaic panel," Appl. Energy, DOI: 10.1016/j.apenergy.2010.01.016, vol. 87, no. 7, pp. 2340–2351, 2010.

[13] M. F. Ishraque, S. A. Shezan, S. J. N. Nur and M. S. Islam.: 'Optimal Sizing and Assessment of an Islanded Photovoltaic-Battery-Diesel Generator Microgrid Applicable to a Remote School of Bangladesh', Engineering Reports, vol. 3, No. 1, p. 12281, 2021.

[14] H. M. Ridha, C. Gomes, H. Hizam, M. Ahmadipour, A. A. Heidari and H. Chen.: 'Multi-objective optimization and multi-criteria decision-making methods for optimal design of standalone photovoltaic system: A comprehensive review', Renewable and Sustainable Energy Reviews, vol. 135, p. 110202, 2021.

[15] T. Tsuji, A. Hidaka and S. Matsumoto, "A stand-alone power supply system using single photovoltaic cell with maximum power point tracking", International Conference on Renewable Energy Research and Applications, Nagasaki, DOI: 10.1109/ ICRERA. 2012. 6477292, pp. 1-5, 2012.

[16] I. M. Opedare, T. M. Adekoya, A. E. Longe, "Optimal Sizing of Hybrid Renewable Energy System for Off-Grid Electrification: A Case Study of University of Ibadan Abdusalam Abubakar Post Graduate Hall of Residence", International Journal of Smart Grid - ijSmartGrid, Vol.4, No.4, December, 2020.

[17] A. Masmoudi, A. Abdelkafi, and L. Krichen, "Electric power generation based on variable speed wind turbine under load disturbance", Energy, vol. 36, no. 8, pp. 5016-5026, 2011.

[18] Y. Saoudi, and H. H. Abdallah, "Contribution of FACTS Device for Persisting Optimal Grid Performance despite Wind Farm Integration", International Review on Modelling and Simulations (I.RE.MO.S.)", vol. 8, no. 2, pp. 1974-9821. 2015.

[19] M. Smaoui, and L. Krichen, "Control, energy management and performance evaluation of desalination unit based renewable energies using a graphical user interface", Energy, vol. 114, pp. 1187-1206, 2016.

[20] R.S.C. Yeung, H.S.H. Chung, N.C.F. Tse, and S.T.H. Chuang, "A global MPPT algorithm for existing PV system mitigating suboptimal operating conditions", Solar Energy, vol. 141, pp. 141-145, 2017.

[21] R. B. Ammar, M. B. Ammar, A. Oualha, "Photovoltaic power forecast using empirical models and artificial intelligence approaches for water pumping systems", Renewable Energy, vol. 153, pp. 1016-1028, 2020.

[22] H. Rezk, M. Al-Dhaifallah, Y.B. Hassan, and H. A. Ziedan, "Optimization and Energy Management of Hybrid Photovoltaic-Diesel-Battery System to Pump and Desalinate Water at Isolated Regions", IEEE ACCESS, pp. 102512-102529, 2020.

[23] M. B. Ammar, M. A. Zdiri, R. B. Ammar, "Fuzzy Logic Energy Management Between Stand-Alone PV Systems", International Journal of Renewable Energy Research, vol. 11, no.3, September, 2021.

[24] A. Y. Hatata, G. Osman and M. M. Aladl, "An optimization method for sizing a solar/wind/battery hybrid power system based on the artificial immune system", Sustainable energy technologies assessments, vol. 27, pp. 83–93, 2018.

[25] R. Kallel, G. Boukettaya, and L. Krichen, "Demand side management of household appliances in stand-alone hybrid photovoltaic system", Renewable Energy, DOI: 10.1016/j.renene.2015.03.024, vol. 81, pp. 123-135, 2015.

[26] Y. Kadri, M. Ben Ammar, and H. H. Abdallah, "Modeling and simulation of DSPMSG power generator connected to grid", 16th International Conference on Sciences and Techniques of Automatic Control and Computer Engineering (STA), IEEE, 2015.

[27] A. Belkaid, I. Colak, and K. Kayisli, "A comprehensive study of different photovoltaic peak power tracking methods," 6th International Conference on Renewable Energy Research and Applications (ICRERA), San Diego, CA, 5-8 Nov, pp. 1073-1079, 2017.

[28] A. I. Nusaif and A. L. Mahmood, "MPPT Algorithms (PSO, FA, and MFA) for PV System Under Partial Shading Condition, Case Study: BTS in Algazalia, Baghdad", International Journal of Smart Grid-ijSmartGrid, vol. 4, No. 3, pp. 100-110, 2020.

[29] M. Rawal, S. Kumar Singh, "Analysis of Droop in PQ Control Mode for Appropriate Power Sharing of Parallel Connecting Inverters", 2nd International Conference for Emerging Technology (INCET) Belgaum, India. May 21-23, 2021.

[30] A. Saidi, A. Harrouz, I. Colak, K. Kayisli, R. Bayindir, "Performance Enhancement of Hybrid Solar PV-Wind System Based on Fuzzy Power Management Strategy: A Case Study", 2019 7th International Conference on Smart

[31] Ur. Ateeq, Z. Elavarasan, R. M. Hafeez, G. Khan, I. Shafiq, & H. H. Alhelou, "An optimal power usage scheduling in smart grid integrated with renewable energy sources for energy management", IEEE Access 9, pp. 84619-84638. 2021.

[32] M. F. Elmorshedy, M. R. Elkadeem, and al. "Optimal design and energy management of an isolated fully renewable energy system integrating batteries and

supercapacitors", Energy Conversion and Management, vol. 245, 114584. 2021.

[33] M. A. Zdiri, T. Guesmi, B. M. Alshammari, K. Alqunun, A. Almalaq, F. Ben Salem H. H. Abdallah and A. Toumi, "Design and Analysis of Sliding-Mode Artificial Neural Network Control Strategy for Hybrid PV-Battery-Supercapacitor System", Energies, vol. 15, no.11, p. 4099, 2022.

[34] A. Al Kassem, M. Al Ahmadi, A. Draou, "Modeling and Simulation Analysis of a Hybrid PV-Wind Renewable Energy Sources for a Micro-Grid Application 2021", 9th International Conference on Smart Grid (icSmartGrid), 2021.